# Effect of Nanoconfinement on the Glass Transition Temperature of Ionic Liquids



| | |
|---|---|
| Journal: | *Physical Chemistry Chemical Physics* |
| Manuscript ID | CP-COM-10-2018-006479.R1 |
| Article Type: | Communication |
| Date Submitted by the Author: | 23-Nov-2018 |
| Complete List of Authors: | Zuo, Yuchen ; University of Akron<br>Zhang, Yuanzhong; University of Akron, Department of Polymer Engineering<br>Huang, Rundong ; University of Akron, Polymer Engineering<br>Min, Younjin; University of Akron, Polymer Engineering |
| | |

PCCP

COMMUNICATION

# Effect of Nanoconfinement on the Glass Transition Temperature of Ionic Liquids

Yuchen Zuo,[a] Yuanzhong Zhang,[a] Rundong Huang[a] and Younjin Min*[a]

Received 00th January 20xx,
Accepted 00th January 20xx

DOI: 10.1039/x0xx00000x

www.rsc.org/

**This work is concerned with investigating the glass transition behavior of ionic liquids as a function of nanoconfinement. The glass transition temperature was found to increase with decreasing confinement length, below a critical confinement of 40–50 nm and 80–90 nm for 1-butyl- 3-methylimidazolium tetrafluoroborate and 1-methyl- 3-octylimidzolium tetrafluoro-borate between alumina surfaces, respectively.**

Ionic liquids (ILs), which are organic salts consisting entirely of ions with a melting point below 100 °C, have recently received an increasing attention from the scientific community owing to their intriguing properties such as negligibly low vapor pressure, fire resistance, tuneable polarity and phase behaviour, excellent chemical and thermal stability, and wide electrochemical windows[1,2]. These beneficial properties of ILs have resulted in their implementations and considerations in catalysis, chemical separation, hazardous chemical storage and transportation, battery technologies, supercapacitors, fuel cells, dye sensitized solar cells, thermo-electrochemical devices, lubrication, thermal storage, carbon dioxide capture and separation, and their applications continue to expand[3,4]. Many of these applications involve the utilization of IL thin films or nanoconfined ILs rather than bulk solvent. For instance, when used as electrolytes, ILs are to transport ions across nanoporous channels of electrodes[5]. IL lubricants are utilized to protect sliding surfaces against wear and damage and to decrease the coefficient of friction at varying loads, some of which can result in surface separations less than a few hundred nanometers[6,7]. In IL-based dye-sensitized solar cells, the photoanode involves a nanostructured wide band-gap semiconductor that is coated with a monolayer of organometallic or organic dye in a thin film geometry[8,9]. ILs mediate the electron transport between the active nanostructured surface and the cathode.

The glass transition temperature ($T_g$), the onset of extensive molecular mobility and long-range transport, is an important property influencing the function, performance, and operational range of thin film devices. Glass transitions are often characterized with very sluggish liquid dynamics induced by the formation of cooperatively rearranging regions (CRRs) with reduced local entropy[10–12]. The length scale of CRRs has been calculated/measured to be in the order of 1–4 nm via the random first-order transition theory of glasses[11], nuclear magnetic resonance (NMR) studies[10], and atomic force microscopy (AFM) technique monitoring polarization fluctuations[13].

Prior studies with simple fluids and polymers revealed $T_g$ under nanoconfined geometries deviates from that under the bulk conditions[14–18]. The critical characteristic length below which there exists a difference between $T_g$ under confined and bulk conditions signifies the onset of the breakdown of continuum behaviours in glass transition. For simple organic liquids, the critical confinement giving rise to noticeable shifts in $T_g$ (>1 °C) ranges from several to several tens of nanometres (< 75 nm)[19–21]. For polymers, confinement levels below 100 nm tend to result in deviations in the glass transition temperature compared to bulk[22,23]. Such deviations are ascribed to a combination of phenomena: the increased relative contribution of the interfacial effects (i.e., liquid-solid or liquid-gas interface associated with confinement) to the free energy of the system[24]; the overlap of the density distribution function of molecules/macromolecules leading structural frustrations and orientational transitions to minimize the potential of mean force under nanoconfinement[25]; changes in the size of CRRs under confinement[21]; and confinement-induced entropy loss[26]. As film thickness and confinement length scale decreases, a decrease or increase in the glass transition temperature has been observed in the literature for various simple fluids and polymers[22,25], governed by the interplay among the abovementioned effects. While there exists a large body of

[a] Department of Polymer Engineering, University of Akron, Akron, Ohio, 44325, USA
[b] Email: ymin@uakron.edu, younjinmin@gmail.com

Electronic Supplementary Information (ESI) available: Materials, details of preparation of nanoporous templates, infiltration of ILs into templates, differential scanning calorimetry measurements. See DOI: 10.1039/x0xx00000x

literature on nanoconfinement effects on the glass transition temperature of simple fluids and polymers, similar studies focusing on ILs are lacking.

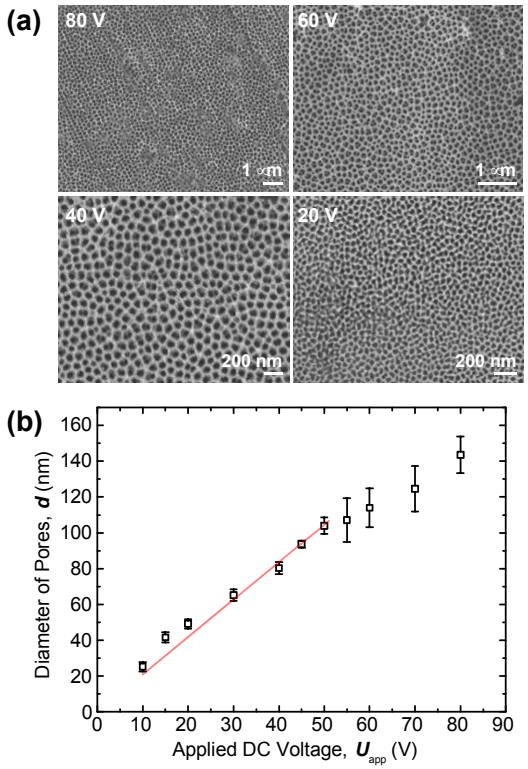


Fig. 1 (a) Representative SEM micrographs of porous anodic alumina (PAA) membranes prepared via a two-step anodization. (b) The relationship between the mean pore diameter, $d$ and bias voltage, $U_{app}$. The red line represents the best linear fit of the experimental data (square symbols).

This work is aimed at determining the confinement length scale below which the glass transition temperature deviates from the one measured in bulk for ILs and whether ILs display a depression or an enhancement in the glass transition temperature under nanoconfined geometries and gaining insights into the interfacial processes controlling the critical confinement length for ILs. To this end, we have relied on nanoporous templates of very systematically varied pore size in modulated differential scanning calorimetry (MDSC) studies with two types of ionic liquids (1-butyl-3-methylimidazolium tetrafluoroborate, $[C_4mim^+][BF_4^-]$ and 1-methyl-3-octyl-imidzolium tetrafluoroborate, $[C_8mim^+][BF_4^-]$).

To derive unambiguous correlations between the nanoconfinement level (pore size) and $T_g$, it is crucial to utilize templates with a narrow size distribution having a small coefficient of variation (i.e., the ratio of the standard deviation to the mean). For this purpose, porous anodic alumina (PAA) membranes were prepared using a two-step anodization process[27] (see *ESI* for details). Fig. 1a displays scanning electron microscopy (SEM) micrographs of nanoporous templates as a function of bias DC voltage. A linear relationship between the applied voltage and the mean pore diameter was observed below 50 V while a sublinear behaviour became noticeable at higher voltages ($U_{app}$ > 50 V) (Fig. 1b). Such a linear trend can be explained via electric field enhanced electrochemical reactions at the electrolyte/alumina and alumina/aluminium interfaces[28]. For large electric fields, ion mobility is sterically hindered by the crowding effect[29], which may account for the sublinear behaviour.

After preparing nanoporous templates of systematically varied sizes, we filled these nanotemplates with $[C_4mim^+][BF_4^-]$ or $[C_8mim^+][BF_4^-]$ for thermal characterization using MDSC. The $T_g$ under bulk condition was measured to be 178.7±0.2 K and 187.2±0.2 K for $[C_4mim^+][BF_4^-]$ and $[C_8mim^+][BF_4^-]$, respectively (Fig. 2). The $T_g$ shifted to higher temperatures when the degree of nanoconfinement increases (the pore size decreases) for both types of ILs. The shift in $T_g$ was more pronounced for the case of $[C_8mim^+][BF_4^-]$. To better understand the relationships between $T_g$ and the confinement length, the glass transition temperature was determined from the first derivative of the MDSC curves shown in Fig.2 and plotted against the pore diameter (Fig. 3).

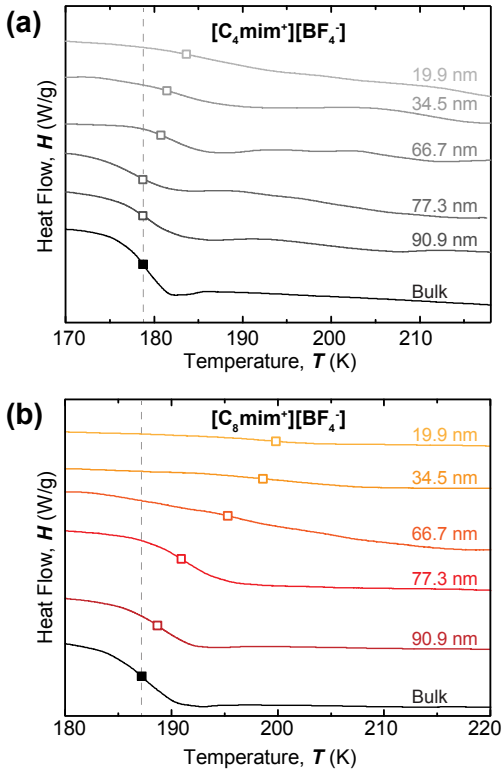


Fig. 2 Heat flow, $H$, versus temperature, $T$, obtained from MDSC for (a) [C4mim+][BF4-] and (b) [C8mim+][BF4-] infiltrated into PAA membranes with systematically varied pore sizes: ; 90.9 nm, 77.3 nm, 66.7 nm, 34.5 nm, 19.9 nm and bulk. Filled black symbols indicate $T_g$ under bulk condition while empty symbols represent shifted $T_g$ under nanoconfinement. The $T_g$ values were determined from the first derivative of each curve and marked accordingly.

The maximum shift in $T_g$ was 4.3 K for $[C_4mim^+][BF_4^-]$ while it was 12.5 K for $[C_8mim^+][BF_4^-]$. The critical distance below which the nanoconfined ILs deviated from bulk ILs in terms of the glass transition temperature ($d_{critical}$) was about 40–50 nm and 80–90 nm for $[C_4mim^+][BF_4^-]$ and $[C_8mim^+][BF_4^-]$, respectively.

The increase in the glass transition temperature can be attributed to the strong attractive interactions between alumina, which bears a positive surface potential in polar solvents, and charged building blocks of ILs, i.e. $[BF_4^-]$. The

attractive interactions favour a closer packing of molecules (i.e., more ordered configuration) in the proximity to the confining surfaces to minimize the free energy of the system. The fact that for a given degree of confinement, the larger shifts were observed in $T_g$ of [$C_8$mim$^+$][$BF_4^-$] compared to that of [$C_4$mim$^+$][$BF_4^-$] is presumably owing to the size effect ([$C_8$mim$^+$] is 17.2 Å × 5.5 Å versus [$C_4$mim$^+$] 11.4 Å × 5.5 Å. See Fig. 3). When confined into the spacing corresponding to several numbers (layers) of ion pairs between solid surfaces, ILs can behave very differently from the bulk, exhibiting oscillatory forces induced by the overlap of the density distribution function[30–33]. The decay distance of oscillatory forces increases with increasing molecular dimension. Hence, for a fixed length scale, the larger molecules can experience the stronger orientational organization upon confinement. However, the critical confinement length below which the continuum behaviour of $T_g$ breaks down is still much larger than the range of oscillatory forces. It is reasonable to consider another length scale controlling the molecular ordering of ILs near the charged surface: i.e. the Debye Length. In our recent studies with the surface forces apparatus, we measured the Debye length of [$C_4$mim$^+$][$BF_4^-$] or [$C_8$mim$^+$][$BF_4^-$] to be 13.3±1.0 nm and 19.2±0.5 nm, respectively (manuscript under review). Given that the $d_{critical}$ corresponds to only a few multiples of the Debye length, it is likely that the Debye length has a stronger control over the critical confinement distance.

We also note that some prior publications reported that there are two glass transition temperatures for nanoconfined supercooled fluids: one is associated with the confined molecules located at distances greater than the range of oscillations in the radial distribution function away from the surface and another is associated with the confined molecules located at distances that smaller than the range of oscillations in the radial distribution function away from the surface [34,35]. For most ionic liquids, the range of oscillations in the radial distribution function away from the surface is less than 5 nm [35,36]. The minimum confinement gap (i.e. pore size of PAA membrane) we used in this study is about 20 nm. Hence, the amount of confined molecules present "in the interfacial region near the confining surface, displaying the interfacial effects" becomes relatively small compared to that of the molecules present "away from the confining surface, lacking the interfacial effects". Hence, considering this relative mass/volume ratio of ILs present near and away from the confining surfaces, it would be challenging to clearly distinguish and assign two separate $T_g$ peaks in this study.

Our key findings can be summarized as follows: The glass transition temperature of ILs increases with decreasing confinement length. The smaller molecules experience a smaller confinement-induced shifts in the glass transition temperature for a given degree of confinement. The critical confinement length below which there exists a deviation in the glass transition temperature between under confined and bulk conditions is about 40–50 nm and 80–90 nm for [$C_4$mim$^+$][$BF_4^-$] and [$C_8$mim$^+$][$BF_4^-$], respectively, between the confining porous anodic alumina surfaces.

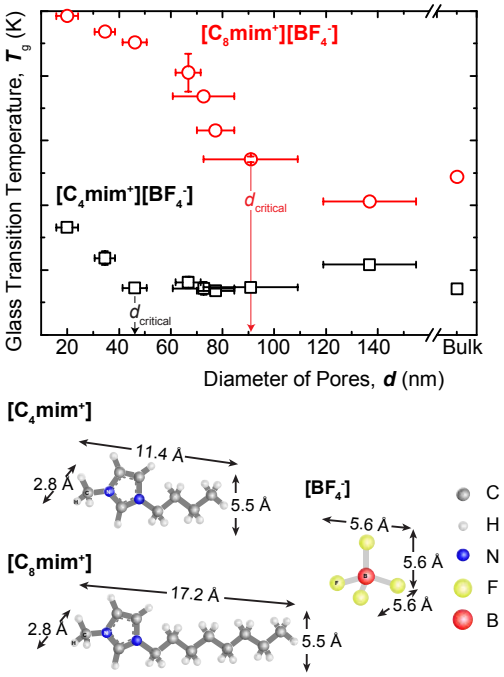


Fig. 3 Glass transition temperature identified from heat flow *versus* temperature curves for [C4mim+][BF4-] and [C8mim+][BF4-] infiltrated into PAA membranes. The $d_{critical}$ indicates the critical distance below which the glass transition behaviors of nanoconfined ILs deviate from the ones in bulk. Chemical structures and approximate ion dimensions of the ILs investigated in this study are shown on the bottom of the graph.

## Acknowledgements

Y.M., R.H, Y.Z., and Y.C. acknowledge funding form National Science Foundation (NSF-CBET Award No. 1511626) and American Chemical Society (ACS PRF Award No. 55789-DNI10).

## Conflicts of interest

There are no conflicts to declare.

## Notes and references

1 T. D. Ho, C. Zhang, L. W. Hantao and J. L. Anderson, *Anal. Chem.*, 2013, **86**, 262–285.

2 T. Torimoto, T. Tsuda, K. Okazaki and S. Kuwabata, *Adv. Mater.*, 2010, **22**, 1196–1221.

3 D. R. MacFarlane, N. Tachikawa, M. Forsyth, J. M. Pringle, P. C. Howlett, G. D. Elliott, J. H. Davis, M. Watanabe, P. Simon and C. A. Angell, *Energy Environ. Sci.*, 2014, **7**, 232–250.

4 G. G. Eshetu, M. Armand, H. Ohno, B. Scrosati and S. Passerini, *Energy Environ. Sci.*, 2016, **9**, 49–61.

5 M. Galiński, A. Lewandowski and I. Stępniak, *Electrochim. Acta*, 2006, **51**, 5567–5580.

6 F. Zhou, Y. Liang and W. Liu, *Chem. Soc. Rev.*, 2009, **38**, 2590–2599.

7 H. Kamimura, T. Kubo, I. Minami and S. Mori, *Tribol. Int.*, 2007, **40**, 620–625.

8 S. Ito, S. M. Zakeeruddin, P. Comte, P. Liska, D. Kuang and

M. Grätzel, *Nat. Photonics*, 2008, **2**, 693.

9 F. Fabregat-Santiago, J. Bisquert, E. Palomares, L. Otero, D. Kuang, S. M. Zakeeruddin and M. Grätzel, *J. Phys. Chem. C*, 2007, **111**, 6550–6560.

10 U. Tracht, M. Wilhelm, A. Heuer, H. Feng, K. Schmidt-Rohr and H. W. Spiess, *Phys. Rev. Lett.*, 1998, **81**, 2727.

11 J. D. Stevenson, J. Schmalian and P. G. Wolynes, *Nat. Phys.*, 2006, **2**, 268.

12 M. Mézard and G. Parisi, *J. Phys. Condens. Matter*, 1999, **11**, A157.

13 E. V. Russell and N. E. Israeloff, *Nature*, 2000, **408**, 695.

14 D. Hudzinskyy, A. V Lyulin, A. R. C. Baljon, N. K. Balabaev and M. A. J. Michels, *Macromolecules*, 2011, **44**, 2299–2310.

15 Y. Rharbi, *Phys. Rev. E*, 2008, **77**, 31806.

16 R. J. Lang and D. S. Simmons, *Macromolecules*, 2013, **46**, 9818–9825.

17 M. D. Ediger and J. A. Forrest, *Macromolecules*, 2013, **47**, 471–478.

18 C. J. Ellison, M. K. Mundra and J. M. Torkelson, *Macromolecules*, 2005, **38**, 1767–1778.

19 C. L. Jackson and G. B. McKenna, *J. Non. Cryst. Solids*, 1991, **131**, 221–224.

20 G. Barut, P. Pissis, R. Pelster and G. Nimtz, *Phys. Rev. Lett.*, 1998, **80**, 3543.

21 S. H. Anastasiadis, K. Karatasos, G. Vlachos, E. Manias and E. P. Giannelis, *Phys. Rev. Lett.*, 2000, **84**, 915.

22 J. A. Torres, P. F. Nealey and J. J. De Pablo, *Phys. Rev. Lett.*, 2000, **85**, 3221.

23 K. Fukao and Y. Miyamoto, *Phys. Rev. E*, 2000, **61**, 1743.

24 M. Alcoutlabi and G. B. McKenna, *J. Phys. Condens. Matter*, 2005, **17**, R461.

25 J. D. McCoy and J. G. Curro, *J. Chem. Phys.*, 2002, **116**, 9154–9157.

26 P. K. Gupta and J. C. Mauro, *J. Non. Cryst. Solids*, 2009, **355**, 595–599.

27 J. H. Yuan, F. Y. He, D. C. Sun and X. H. Xia, *Chem. Mater.*, 2004, **16**, 1841–1844.

28 Z. Su and W. Zhou, *Adv. Mater.*, 2008, **20**, 3663–3667.

29 M. S. Kilic, M. Z. Bazant and A. Ajdari, *Phys. Rev. E*, 2007, **75**, 21502.

30 S. Perkin, L. Crowhurst, H. Niedermeyer, T. Welton, A. M. Smith and N. N. Gosvami, *Chem. Commun.*, 2011, **47**, 6572–6574.

31 D. Wakeham, R. Hayes, G. G. Warr and R. Atkin, *J. Phys. Chem. B*, 2009, **113**, 5961–5966.

32 Y. Min, M. Akbulut, J. R. Sangoro, F. Kremer, R. K. Prud'homme and J. Israelachvili, *J. Phys. Chem. C*, 2009, **113**, 16445–16449.

33 J. Wu, T. Jiang, D. Jiang, Z. Jin and D. Henderson, *Soft Matter*, 2011, **7**, 11222–11231.

34 G. B. McKenna, *Le J. Phys. IV*, 2000, **10**, Pr7-53.

35 R. Richert, *Annu. Rev. Phys. Chem.*, 2011, **62**, 65–84.

36 C. S. Perez-Martinez, A. M. Smith and S. Perkin, *Phys. Rev. Lett.*, 2017, **119**, 26002.